

UDC 658.5: 004  
JEL L60, L69, O33, D24

## DIGITAL PROGRAM CONTROL AND COMPLEX COMPONENT PROCESSING IN PERFORMANCE- DRIVEN PRODUCTION ENGINEERING

**Desislava Petrova \***  
Technical University of Gabrovo,  
Gabrovo, Bulgaria  
ORCID iD: 0000-0002-8970-5722

**Ivelina Balabanova**  
Technical University of Gabrovo,  
Gabrovo, Bulgaria  
ORCID iD: 0000-0002-0835-1732

**Georgi Georgiev**  
Technical University of Gabrovo,  
Gabrovo, Bulgaria  
ORCID iD: 0000-0001-5130-8652

\*Corresponding author  
E-mail: des\_petrova@abv.bg

**Received:** 12/08/2025  
**Revised:** 20/11/2025  
**Accepted:** 16/12/2025

DOI: 10.61954/2616-7107/2025.9.4-9

© Economics Ecology Socium, 2025  
CC BY-NC 4.0 license

**Introduction.** Modern mechanical engineering is characterised by a constant increase in the proportion of parts with complex configurations (bodies of revolution with rectilinear and curvilinear elements) manufactured using materials with special physical and mechanical properties. The production of such complex components requires high precision, flexibility, and efficiency. The complex shape and variety of technological manufacturing processes are most effectively determined by their efficient processing on automated multifunctional equipment with a central processing unit (CPU).

**Aim and tasks.** This study aims to investigate the processing of complex-shaped details made of difficult-to-process materials on Computer Numerical Control (CNC) or CNC machining is the automated control of machine tools by a computer lathes to increase the efficiency of the technological process.

**Results.** The efficiency of the technological process has been increased when processing complex-shaped parts made of difficult-to-process materials on CNC lathes, as a methodology has been developed for determining cutting modes using the criterion of “processing productivity”. The main task at the technological preparation stage of production is optimisation in determining the parameters of the cutting mode, based on the criterion of “durability at maximum productivity”. In the developed methodology for determining the cutting mode, the volume of material removed per unit time is used as a criterion for “processing productivity”, while simultaneously taking into account the relationship between  $a_p$ ,  $f$ , and  $v_c$  through the cutting power and tool durability, which allows an increase in productivity of up to 74%. Multi-pass roughing is more effective for CNC lathes than single-pass, and maximum cutting productivity is achieved at maximum tool feed.

**Conclusions.** The analysis showed that productivity gains from increasing the cutting depth are limited by machine power. Optimisation based on the “tool life at maximum productivity” criterion is effective only when the machine power is not a limiting factor. It was found that reducing the target tool life ( $T$ ) does not always increase productivity. Reducing  $T$  is effective only in conditions where higher cutting speeds do not exceed the available machine power; otherwise, the actual tool life may even increase. The optimisation of  $T$  must consider machine power limitations: reducing  $T$  is effective only when higher cutting speeds do not exceed the permissible power.

**Keywords:** Control Design, Engineering Computing, Productivity, Mechanical Systems, Production Engineering.

## 1. Introduction.

In the digitalisation and production automation age, many indicators accompanying many business processes in an organisation are changing in real time (Aguiar et al., 2022; Demirova & Mehmedov, 2023; Mnzool et al., 2024). To ensure the continuity of the processing of the part, an organised set of interconnected technical and electronic tools is required, including computer technologies and various software products (Maropoulos, 2003).

In technology, along with cylindrical and flat surfaces, various curvilinear surfaces are also widely used, united under the general name profile (Damianov & Demirova, 2018). The details of such surfaces form the group of details with a complex shape (handles, profile shafts, copiers, rolling and calibrating machine shafts, pulleys for flat and V-belts, wagon axles and tyre wheels, profile circular knives and cutters, etc.).

The most common types of profile surfaces are rotational, formed by a curvilinear movement along a guiding circle.

All cylindrical parts (smooth and stepped) are a special case of parts with complex shapes, and the situations related to the technologies for processing parts with complex shapes can be referred to as technologies for processing cylindrical parts (Harris & Meyers, 2019).

Bearing this in mind, it is clear that the class of parts with a complex rotational shape appears to be very extensive, unites a significant number of names of various machine-building parts from all branches of industry, and in connection with this, the processing of parts of this class occupies a significant place in operations for mechanical processing.

Parts with complex rotational shapes are primarily processed on lathes, making studying the forming process an important technical and economic task. This process is especially relevant in the conditions of partial production automation, characterised by the use of CNC machines and other expensive automated equipment, which creates prerequisites for risk (Racz et al., 2020; Soori et al., 2024).

## 2. Literature Review.

### 2.1. Formation of Complex Profiled Surfaces.

The surfaces defining the geometric shapes of the objects surrounding us are diverse and endless, accompanied by the digitalisation of the production process (Dahmani et al., 2021; Demirova & Mehmedov, 2023). There are different ways of specifying surfaces. In mathematics, a surface is considered a geometric locus of points whose coordinates satisfy a given equation of  $F(x, y, z) = 0$ , where  $F(x, y, z)$  is a polynomial of  $n$ th power or some transcendental function. The surface can be set skeletal (framework), which is considered a set of lines belonging to it.

The surface can also be considered a set of consecutive positions of a line that moves in space according to a certain law. This is the so-called kinematic way of forming and setting the surface.

The process of forming a surface using a kinematic approach to define it, as well as the main concepts related to it, are explained with reference to the example in Fig. 1.

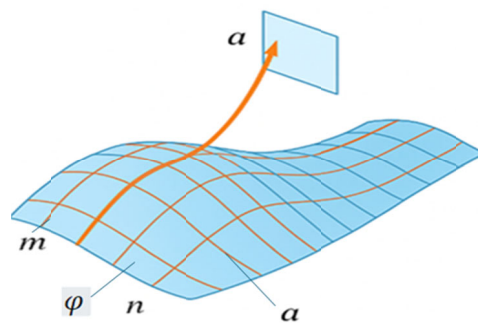


Fig. 1. The Process of Forming a Surface.

The surface  $\varphi$  is obtained by sliding a straight line  $a$  along two spatial curved lines  $m$  and  $n$ , with line  $a$  remaining parallel to plane at any moment. The moving line forming the surface is called forming, and the fixed lines  $m$  and  $n$  and planes  $a$ .

These geometric elements and their relationships, representing independent conditions uniquely defining a surface, are called surface determinants. Computer simulations have already been implemented in all spheres of engineering activities. An ever-increasing range of objects and phenomena is subject to computer modelling (Durán, 2018).

The kinematic way of forming surfaces, which is very convenient for use in engineering practice, where the geometric shapes of objects are depicted and set graphically, is embedded as an ideology in modern Computer Aided Design (CAD) systems for graphic 3D modelling. Each object is constructed or drawn using a CAD system as a CAD model.

This model is built upon an existing foundation of geometric elements used in computer-generated images. This study aims to develop a morphological matrix of the determinants of surfaces from the standpoint of the kinematic way of their formation, and the constructed system-morphological approach to their formation creates conditions for a theoretical analysis of the formed surfaces.

The same surface can be formed through different methods. When setting the determinant of a surface, one should proceed from the kinematic approach of its formation (Waldron & Schmiedeler, 2016).

For example, Figure 2 shows the formation of a cylindrical surface  $\varphi$  in three different kinematic ways. In the first case, the surface is formed during the progressive movement of line  $a$  along guide  $t$  (arc of a circle). The determinant of the surface consists of a geometric part forming  $a$ , guiding  $t$ , and movement of the forming progressive.

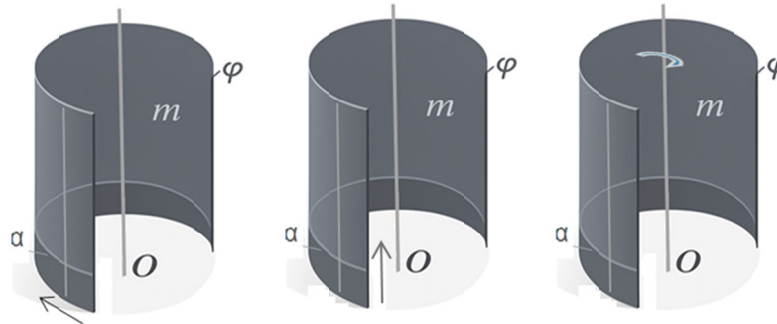


**Fig. 2. Forming a Cylindrical Surface  $\varphi$  in Different Kinematic Ways.**

In the second case, the surface is formed during the progressive movement of the arc from circle  $a$  in the direction of guiding line  $t$ .

The determinant of the surface consists of a geometric element, the forming line ( $a$ ), a guiding element, the guide line ( $t$ ), and the movement of the forming element, which is progressive.

In the third case, the surface is generated by the rotational movement of line  $a$  around line  $t$ . The determinant of the surface includes a geometric component that directs the rotational motion of the formed part.

The determinant of each surface consists of the following main parts: geometry, which represents a set of lines with which the forming and guiding lines are set, and the law of motion of the former in forming the surface.

## 2.2. Differential-Morphological Approach in Surface Formation.

The main geometric element of a surface is its constituent element. It can be a curved or straight line, plane, or spatial, which, when moved in space, forms a nonlinear or linear surface, respectively.

Alternatives for the formant geometry are presented in the first column of the morphological table of surface determinants (Table 1).

In the kinematic way of forming, the surface is considered a set of all positions of the former, which can remain constant in shape or change while forming the surface. Surfaces with a shape changer in motion are identical to surfaces defined by a continuous skeleton, and their shaping is not considered.

Therefore, the morphological Table 1 has no alternatives for formations with such geometries. These surfaces include the so-called channel surfaces, which are considered to be formed by a continuous skeleton of closed plane sections.

These sections are oriented in space in a certain way and have a shape and face that change according to a particular law (Matsson, 2025). The law of displacement of the former in the formation of the surface can be set graphically in the form of a family of guide lines  $t$ ,  $n$ , and  $l$ . It can be defined with two guide lines and a guide plane to perform the function of the third guide line. Alternatives for surface guidelines are presented in column 2, and the guide plane in column 3 of the morphological table of determinants. Most often, the law of motion during surface formation is such that the formation line slides along a guide line, with an additional condition specifying the movement of the formation (column 4 of Table 1).

**Table 1. Morphological Table of Surface Determinants.**

1. Generatrix ( $M_g$ )	Law of Forming Movement ( $M_{lm}$ )		
	2. Guideline ( $m$ ) 3. Guideline ( $n$ ) 4. Guideline ( $l$ )	5. Guide plane ( $a$ )	6. Movement of the forming
1.1. <i>Straight line</i>	2.3 or 4.1. <i>Straight line</i> 2.3 or 4.2. <i>Point (Dot)</i>	5.1. Front projection 5.2. Horizontal projection 5.3. Profile projection 5.4. In general position - set with a point and a line not passing through the point 5.5. Normal plane 5.6. Rectifiable plane 5.7. Ossular plane 5.8. There is no	6.1. Gradually 6.2. Rotating 6.3. Screw 6.4. Sliding 6.5. Drag by point 6.6. Something else 6.7. There is no
<i>A flat curved line:</i> 1.2. District 1.3. Ellipse 1.4. A parable 1.5. Hyperbole 1.6. Another algebraic equation 1.7. Transcendent equation 1.8. Polygon 1.9. Free	<i>A flat curved line:</i> 2.3 or 4.3. District 2.3 or 4.4. Ellipse 2.3 or 4.5. A parable 2.3 or 4.6. Hyperbole 2.3 or 4.7. Another equation 2.3 or 4.8. A polygon 2.3 or 4.9. Free		
<i>Spatial curve line:</i> 1.10. Algebraic equation 1.11. Transcendent equation 1.12. Free	<i>Spatial curve line:</i> 2.3 or 4.10. Algebraic equation 2.3 or 4.11. Transcendent equation 2.3 or 4.12. Free 2.3 or 4.13. There is no		

The morphological table of determinants considering the shape of the forming element and the law of its movement when forming the surface can be considered as two morphological tables joined together:

- Forming –  $M_f$  (column 1 of Table 1).

- The traffic law –  $M_{lm}$  (columns 2-4 of Table 1).

Thus, the morphological matrix of determiners has the following collapsed form:  $M_f = M_g \wedge M_{lm}$  and correspondingly expanded numerical form:

$$M_f = \begin{matrix} 1.1 \\ 1.2 \\ 1.3 \\ 1.4 \\ 1.5 \\ 1.6 \\ 1.7 \\ 1.8 \\ 1.9 \\ 1.10 \\ 1.11 \\ 1.12 \end{matrix} \wedge \begin{matrix} 2.1 & 3.1 & 4.1 & 5.1 & 6.1 \\ 2.2 & 3.2 & 4.2 & 5.2 & 6.2 \\ 2.3 & 3.3 & 4.3 & 5.3 & 6.3 \\ 2.4 & 3.4 & 4.4 & 5.4 & 6.4 \\ 2.5 & 3.5 & 4.5 & 5.6 & 6.5 \\ 2.6 & 3.6 & 4.6 & 5.7 & \\ 2.7 & 3.7 & 4.7 & 5.8 & \\ 2.8 & 3.8 & 4.8 & & \\ 2.9 & 3.9 & 4.9 & & \\ 2.10 & 3.10 & 4.10 & & \\ 2.11 & 3.11 & 4.11 & & \\ 2.12 & 3.12 & 4.12 & & \\ 2.13 & 3.13 & 4.13 & & \end{matrix} \quad (1)$$

The use of the systematic differential-morphological approach to surface formation is illustrated in Figure 3, where the following synthesised surfaces are depicted:

- a) SF1 |1.1|+|2.9-3.13-4.13-5.8-6| (cylindrical surface formed by a straight line moving along a curved guide);
- b) SF2 |1.9|+|2.1-3.13-4.13-5.8-6.2| (rotational surface obtained by the rotation of a curvilinear forming around a rectilinear guide);
- c) SF3 |1.1|+|2.1-3.13-4.13-5.8-6.3| (screw surface obtained by combined rotary and progressive movements of a rectilinear forming around a rectilinear guide);
- d) SF4 |1.1|+|2.9-3.2-4.13-5.8-6.4| (conical surface formed by sliding a straight line along two guides, one being a point);

e) SF5 |1.1|+|2.1-3.5-4.1-5.8-6.4| (doubly bent conoid obtained by sliding a rectilinear forming along three guides, two rectilinear and one parabolic);

f) SF6 |1.1|+|2.1-3.9-4.4-5.8-6.4| (inclined wedge obtained by sliding a straight line forming along three guides in parallel planes, two smooth curves and one straight line).

The graphic implementation of the examples shown was made in the environment of the Computer Aided Design (CAD) system for modelling Solid Works of Dassault Systèmes (Systemes, 2011), which, in terms of its capabilities and tools, is identical to Solid Edge of Unigraphics and Inventor of Autodesk (Harris & Meyers, 2019; Waguespack, 2014).

There is an exact correspondence between the movements of the surface formers from the examples in (Fig. 3a, b, c, d) and the tools used for graphical computer modelling of surfaces, namely extruded, revolved, and swept surfaces.

The last two surfaces (Fig. 3e, f) have a complex shape and can be modelled only by connected sections, setting the final and intermediate positions of the former and the contours of the guides (a loft tool is used).

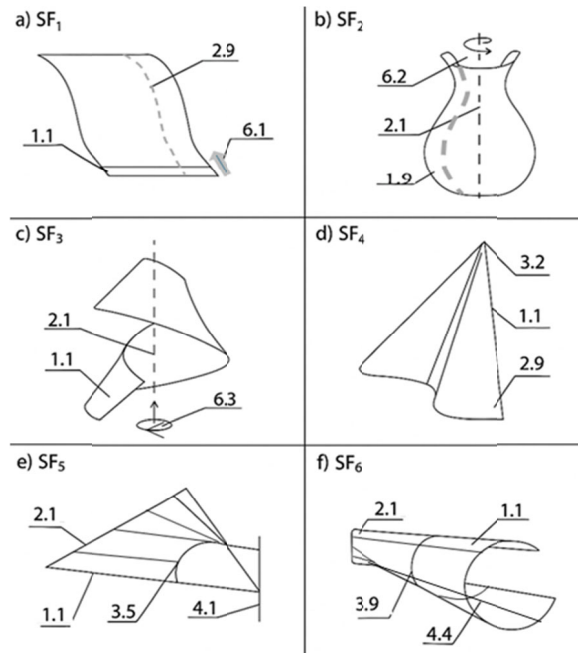


**Fig. 3. A Systematic Differential-Morphological Approach to Surface Formation.**

### 3. Methodology.

This study uses the methodology presented by Krumov (2022), which is part of the classical calculations for determining the cutting conditions in turning operations on metal-cutting machines and those equipped with Computer Numerical Control (CNC). The main machine time in turning, denoted as  $T_{m(m)}$  is determined by the following relation:

$$T_{m(m)} = \frac{L_p}{v_f} \cdot p = \frac{L_p}{f \cdot n_c} \cdot \frac{Z}{a_p}, \text{ min} \quad (2)$$

Where:

$a_p$  – cutting depth of cut, mm;  
 $L_p$  – length of one working stroke of the tool, mm;  
 $V_f$  ( $v_f = f \cdot n_c$ ) feed speed, mm/min;  
 $n_c$  – workpiece rotation frequency,  $\text{min}^{-1}$ ;  
 $p$  – number of working passes ( $p = Z/a_p$ );  
 $Z$  – machining allowance, mm.

Considering the expression for the rotation frequency (Kuzmanov, 2006):

$$n_c = \frac{10^3 \cdot v_c}{\pi \cdot D}, \text{ min}^{-1}$$

where  $D$ , mm – diameter of the workpiece, equation (2) becomes:

$$T_{m(m)} = \frac{L_p \cdot \pi \cdot D}{10^3 \cdot v_c \cdot f} \cdot \frac{Z}{a_p}, \text{ min} \quad (3)$$

The numerator represents the total volume of the machining allowance, and the denominator corresponds to the chip volume removed per minute. To reduce the machine time, it is necessary to increase the parameters appearing in the denominator, namely the cutting speed  $v_c$ , the feed  $f$ , and the depth of cut  $a_p$ . These parameters are interrelated through the equations describing the cutting power and tool life:

$$\begin{cases} P_p = \frac{F_z \cdot v_c}{60 \cdot 10^3} \\ v_c = \frac{C_v \cdot k_v}{T^{m_v} \cdot a_p^{x_v} \cdot f^{y_v}} \\ F_z = C_F \cdot a_p^{x_F} \cdot f^{y_F} \cdot v_c^{m_F} \end{cases} \quad (4)$$

Where:

$P_p$  – cutting power, kW;  
 $T$  – tool life, min;  
 $F_z$  – tangential component of the cutting force, N;  
 $m_v, m_F, x_v, x_F, y_v, y_F$  – exponents;

$C_v, C_F$  – constants;

$k_v$  – coefficient;

$T_{m(m)}$  – machine time, min.

From the analysis of system (4), it follows that for constant cutting power and tool life, any change in one of the parameters requires coordinated adjustments in the other two to maintain a balance between durability and power consumption. This interdependence is essential when choosing rational cutting parameters according to the maximum productivity criterion.

Many studies, however, do not fully consider the interaction among  $v_c$ ,  $f$ , and  $a_p$ . For instance, the productivity criterion is often related solely to the tool life period, neglecting the machine's power limitations. Hoischen and Hesser (2006) suggested reducing the tool life period to 15–25 minutes while proportionally increasing  $v_c$ ; the additional time for tool replacement would be compensated by automated tool change. Nevertheless, this method does not account for the power of the main motion or the mutual dependence of cutting parameters.

The tool life ensuring maximum productivity is expressed as:

$$T_{Pmax} = \frac{(1-m)\tau_{ct}}{m} \quad (5)$$

Where:

$T_{Pmax}$  – the durability providing the greatest productivity;

$\tau_{ct}$  – the tool change time;

$m$  – relative durability index (for carbide tools,  $m = 0.2$ ).

To determine the optimal cutting speed  $v_c$  that provides the greatest productivity, parameters  $a_p$  and  $f$  are first selected, and then  $v_c$  is calculated using equations (4) and (5).

This indicator expresses the material removal rate per unit time and incorporates the interdependence among the cutting parameters. To achieve maximum performance, the product  $v_c$ ,  $f$  and  $a_p$  must be increased, provided that the limits of cutting power  $P_p$  and tool life  $T$  are not exceeded. Hence, the proposed methodology provides a systematic way to select cutting conditions that simultaneously satisfy the technical constraints of the machine and ensure the highest possible machining productivity.

#### 4. Results.

The recalculations for the new tool life  $T = 18 \text{ min}$  and old  $T = 20 \text{ min}$  showed the following:

- When the cutting edge operates in a regime where the machine power is not a limiting factor (low and medium depth of cut  $a_p$ ), reducing the tool life from 20 to 18 minutes allows an increase in cutting speed  $v_c$  according to Taylor's equation  $v \times T^m = \text{const}$ .

- With  $m=0.2$ , this gives approximately +2.13% increase in  $v_c$  and correspondingly in productivity  $P_r$  (volume removed per minute).

- At  $a_p = 0.5 \text{ mm}$  productivity grows from 148.9 to 152.07  $\text{cm}^3/\text{min}$ ; at  $a_p = 1.0 \text{ mm}$ : from 218.1 to 222.75  $\text{cm}^3/\text{min}$ ; and at  $a_p = 1.5 \text{ mm}$ : from 291.4 to 297.61  $\text{cm}^3/\text{min}$ .

- For regimes with higher  $a_p (\geq 2 \text{ mm})$ , the power limitation of the machine ( $P_p = 8 \text{ kW}$ ) remains the controlling factor, so those modes stay unchanged and actual tool life  $T_{\text{act}}$  remains higher than 18 min.

- Reducing  $T$  gives small but measurable productivity gain (+2.1%) in non-power-limited regimes and no change for power-limited ones.

- The comprehensive experimental investigations conducted across a wide range of variations in feed rate ( $f$ ) and depth of cut ( $a_p$ ) revealed a consistent regularity in the variation of the exponents of  $f$  and  $a_p$  within system (4). The experiments encompassed both “straight” and “reverse” chip formation regions. Cutting within the “reverse” chip zone occurs when the auxiliary cutting edge assumes the dominant role in material removal, a condition typically observed when  $f > a_p$ .

- It follows from the solution of the system (4) that for a given cutting power and tool life period, the maximum productivity  $P_r$  is reached at maximum feed (Fig. 4), and in this case  $a_p$  and  $v_c$  can be numerically changed, up to as they are related to  $f$  from the system (4), but under the condition that  $P_p$  and  $T$  do not change.

- It follows from the system (4) that with an increase in  $a_p$ , the cutting performance - falls (Fig. 5) and therefore, when determining (setting) cutting modes, we should not strive to set the maximum possible  $a_p$ .

- For example, the modes of cutting when scraping *Steel 45* were compared, obtained by solving system (4) and according to the traditional methodology.

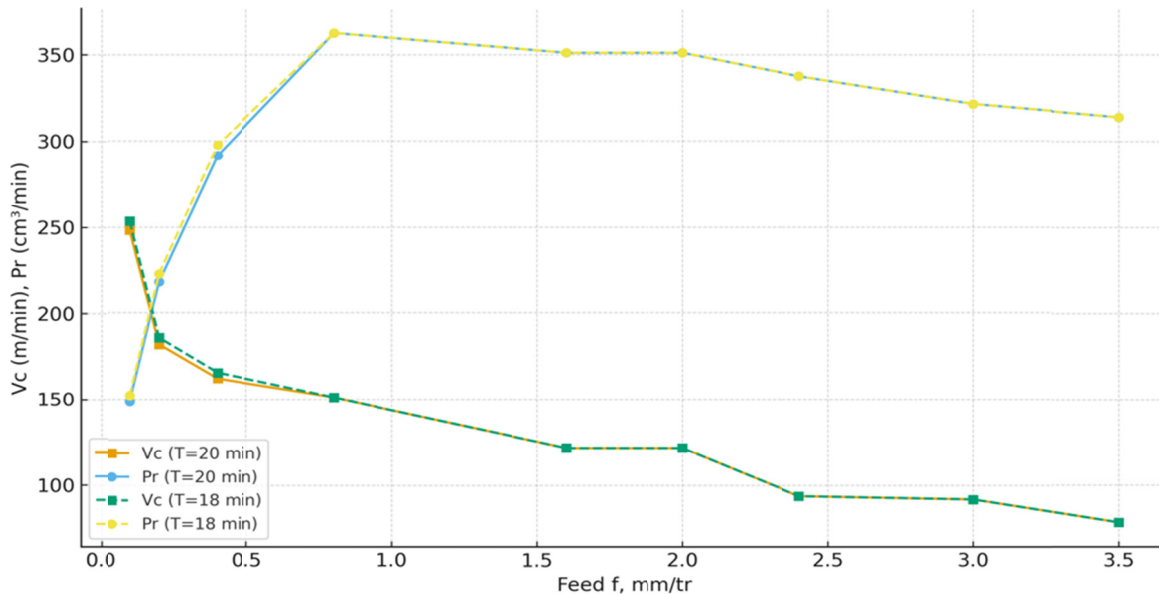
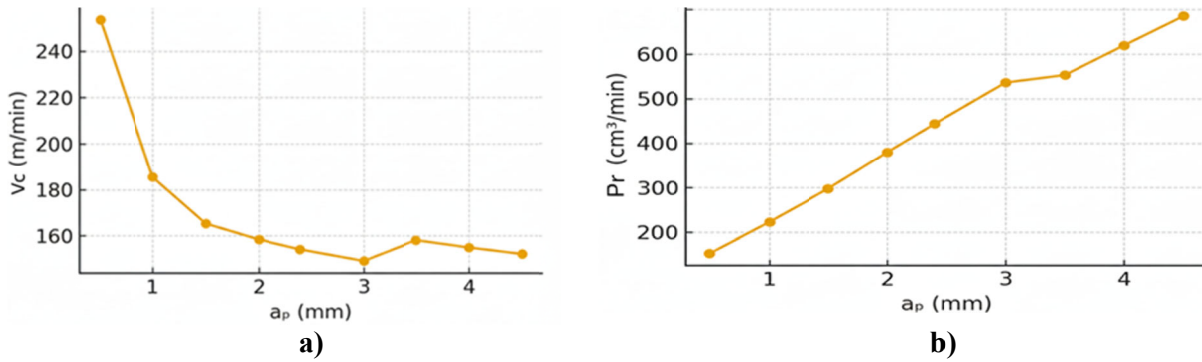


Fig. 4. Correlation of Feed Rate and Main Cutting Parameters.



**Fig. 5. Variation of  $v_c$ ,  $P_r$  and  $f$  on  $a_p$  for Various Processing Conditions: (a) At Low Feed Rate; (b) At High Feed Rate.**

The corresponding graphs (Figures 4 and 6) were constructed to illustrate how the first approach achieves the maximum increase in feed rate  $f$ , while the second ensures the greatest increase in cutting depth  $a_p$ . Figure 4 shows the change in key parameters with increasing feed rate.

Whereas, Figure 5 depicts their behaviour as the cutting depth increases.

Table 2 presents the calculated values of the cutting mode parameters determined according to the conventional methodology, along with their corrections based on the cutting power  $P_p$ .

**Table 2. Cutting Mode Parameters According to the Traditional Method.**

$T_{estimate}$	$P_r$	$v_c$	$P_p$	$a_p$
<i>min</i>	<i>cm³/min</i>	<i>m/min</i>	<i>kw</i>	<i>mm</i>
18.0	152.1	253.5	3.2	0.5
18.0	222.7	185.6	4.8	1.0
18.0	297.6	165.3	6.5	1.5
22.8	362.6	151.1	8.0	2.0
58.1	351.1	121.9	8.0	2.4
182.5	337.5	93.8	8.0	3.0
271.5	321.5	91.9	8.0	3.5
538.7	314.0	78.5	8.0	4.0
986.1	307.6	68.3	8.0	4.5

$T_{estimate}$	$P_r$	$v_c$	$P_p$	$a_p$
<i>min</i>	<i>cm³/min</i>	<i>m/min</i>	<i>kw</i>	<i>mm</i>
20.0	148.9	248.2	3.1	0.5
20.0	218.1	181.7	4.7	1.0
20.0	291.4	161.9	6.4	1.5
22.8	362.6	151.1	8.0	2.0
58.1	351.1	121.9	8.0	2.4
182.5	337.5	93.8	8.0	3.0
271.5	321.5	91.9	8.0	3.5
538.7	314.0	78.5	8.0	4.0
986.1	307.6	68.3	8.0	4.5

The column  $T_{estimate}$  lists the actual tool life values, obtained after adjusting the cutting regime when the power of the main motion exceeded the allowable capacity. The cutting speed was reduced accordingly, resulting in an extended tool life period (Vachev, 1998).

The machining performance, calculated on the basis of the solution to system (4), exhibits an increasing trend with the rise of feed rate. In contrast, the cutting speed ( $v_c$ ) initially decreases as  $f$  increases, and subsequently begins to rise again (Fig. 4).

This behaviour corresponds to the transition of the cutting process into the “reverse” chip formation zone, where the influence of  $f$  on  $v_c$  diminishes.

Consequently, within this region, the effect of increasing  $f$  becomes more pronounced than in the “straight” chip formation zone.

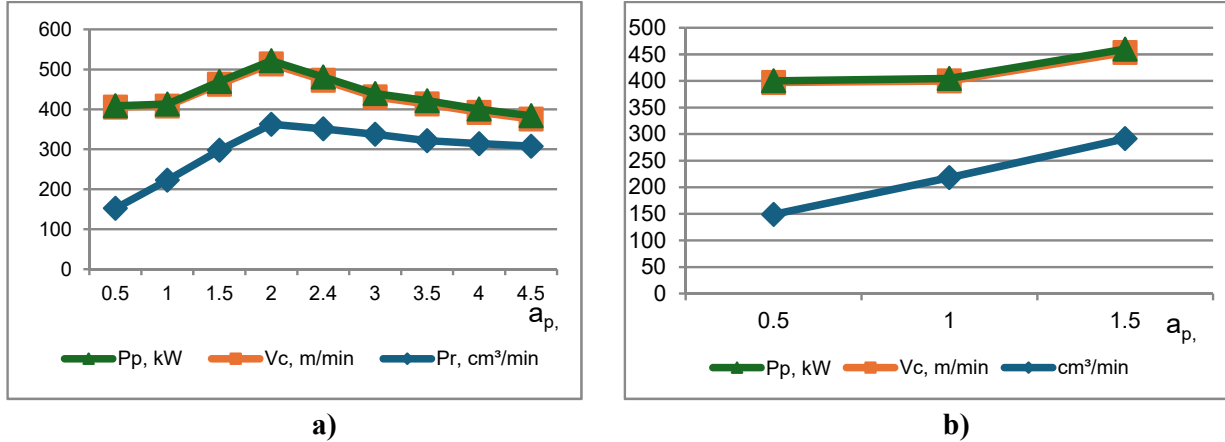


**Fig. 6. Correlation of Key Cutting Parameters  $P_r$ ,  $v_c$  and  $P_p$  with Respect to Depth of Cut  $a_p$ : (a) High-Velocity Zone; (b) Peak Overload Assessment.**

Based on the obtained experimental results, a methodology for selecting optimal cutting parameters is proposed. This approach establishes a relationship between the cutting mode parameters and the technical capabilities of the machine tool and cutting instrument, as expressed in system (4). The procedure begins with setting the maximum feasible feed rate ( $f$ ). After solving system (4), the corresponding cutting speed ( $v_c$ ) and depth of cut ( $a_p$ ) are determined.

Finally, the number of tool passes ( $p$ ) is calculated as the integer part ( $int$ ) of the following expression:

$$p = int\left(\frac{z}{a_p}\right) + 1 \quad (6)$$

Based on the peculiarities of normalising program operations, it can be determined that the time required for processing one detail.

For comparison, the proposed cutting modes according to the developed and traditional methodology for scraping blanks from *Steel45* with a diameter of  $\varnothing 100$  mm to  $\varnothing 80$  mm with a power of the main translation of the machine 8 kW.

In the first case  $t_{ed} = 0,31$  min, and in the second case  $t_{ed} = 0,54$  min. The productivity of the process according to the proposed methodology was 74%.

## 5. Conclusions.

Details with a complex rotational shape are a set of elementary surfaces with rectilinear and curvilinear elements, and their composition can include elementary surfaces of one or more geometric types (cylindrical, frontal, conical, spherical, elliptical, parabolic, etc.). The theoretical analysis of their formation can mathematically describe all elementary rotary surfaces. The movements of the forming and guiding production lines enable the correct solution of tasks related to the technological methods of their production.

There are various technological variants (schemes) for compensating for rough processing when turning details with complex shapes, which makes their processing efficient under partial automation. The analysis of the structural and technological features of details combining complex profile surfaces (shafts, discs, vanes, etc.) shows that their complex shape and the variety of technological processes for manufacturing best determine their effective mechanical processing on automated multi-purpose equipment with a numerically controlled machines. Machining remains the most common method of part fabrication, particularly in aircraft engine manufacturing.

Despite the development and widespread use of small blanking methods and concentrated energy flows for forming. The labour intensity of mechanical operations accounts for 50-60% of the total labour intensity required to produce parts, with machining of the workpiece accounting for 80%. With an increase in the volume of used materials with special physical and mechanical properties manufacturing processes become more complex.

The configuration of details has also become more complicated. The primary task at the stage of technological preparation for production, utilising automated multi-purpose equipment, is to select cutting modes, tool geometry, and other mode conditions, ensuring the efficient operation of expensive lathes for mechanical processing, which is essentially a problem of optimisation.

The analysis of problems associated with selecting modes for mechanical processing reveals that determining the optimal conditions for producing details with complex profile surfaces using automated equipment is a crucial technical and economic task.

There are insufficient works related to creating mathematical models for the mechanical processing process. Their application in solving technological issues is also limited. Additionally, there are no methods for parametric optimisation considering technological limitations. The performed recalculations showed that with a reduction in tool life from  $T = 20$  to  $T = 18$  min, the cutting speed and productivity increase by approximately 2.1%, which confirms the feasibility of optimizing cutting modes in processing zones with unlimited power.

When determining the parameters of the cutting mode based on the criterion “durability at maximum productivity”, in the presence of a limitation on the cutting power, the increase in processing productivity with the increase in the cutting depth is possible only at small depths (at medium and large cutting depths, after adjusting the modes, productivity decreases). For CNC-machines lathes, multi-pass roughing is more efficient than single-pass and maximum cutting performance is achieved at maximum tool feed.

## REFERENCES

- Aguiar, M. F., Mesa, J. A., Jugend, D., Pinheiro, M. A. P., & Fiorini, P. D. C. (2022). Circular product design: strategies, challenges and relationships with new product development. *Management of Environmental Quality*, 33(2), 300–329. <https://doi.org/10.1108/meq-06-2021-0125>
- Damianov, D. & Demirova, S. (2018). Principles of Designing Automated Logistics Systems - Hybrid Component of Cyber-Physical Systems, *International Conference on High Technology for Sustainable Development*. <https://doi.org/10.1109/HiTech.2018.8566533>
- Demirova, S., & Mehmedov, M. (2023). Study of the level of digitalization of logistics activities in small and medium-sized enterprises in the North-East Region. *E3S Web of Conferences*, 402, 01018. <https://doi.org/10.1051/e3sconf/202340201018>
- Durán, J. M. (2018). *Computer Simulations in Science and Engineering: Concepts - Practices - Perspectives*. Springer International Publishing. <https://doi.org/10.1007/978-3-319-90882-3>
- Harris, L. V. A., & Meyers, F. (2019). Engineering design graphics: Into the 21st century. *Engineering Design Graphics Journal*, 71(3), 20-34. <https://doi.org/10.18260/edgj.v71i3.7>
- Hoischen, H., & Hesser, W. (Eds.). (2011). *Technisches Zeichnen: Grundlagen, Normen, Beispiele, Darstellende Geometrie* (33rd ed.). Cornelsen Scriptor.
- Krumov, K. (2022). Processing efficiency research on CNC lathes. In *International Scientific Conference “UNITECH’22”* (pp. 379–383). Technical University of Gabrovo.
- Kuzmanov, T.V. (2006). Machining of complex shaped parts ON CNC lathes. *News of TU-Gabrovo*, 33, 24-29.

- Maropoulos, P. (2003). Digital enterprise technology--defining perspectives and research priorities. *International Journal of Computer Integrated Manufacturing*, 16(7–8), 467–478. <https://doi.org/10.1080/0951192031000115787>
- Matsson, J. E. (2025). *An Introduction to Solidworks Flow Simulation 2025*. SDC publications.
- Mesa, J. A., Gonzalez-Quiroga, A., Aguiar, M. F., & Jugend, D. (2022). Linking product design and durability: A review and research agenda. *Heliyon*, 8(9), e10734. <https://doi.org/10.1016/j.heliyon.2022.e10734>
- Mnzool, M., Almujiabah, H., Bakri, M., Gaafar, A., Elhassan, A. A. M., & Gomaa, E. (2024). Optimization of cycle time for loading and hauling trucks in open-pit mining. *Mining of Mineral Deposits*, 18(1), 18–26. <https://doi.org/10.33271/mining18.01.018>
- Racz, S.-G., Breaz, R.-E., & Cioca, L.-I. (2020). Hazards That Can Affect CNC Machine Tools during Operation—An AHP Approach. *Safety*, 6(1), 10. <https://doi.org/10.3390/safety6010010>
- Soori, M., Jough, F. K. G., Dastres, R. & Arezoo, B. (2024). Robotical Automation in CNC Machine Tools: A Review. *Acta Mechanica et Automatica*, 18(3), 434–450. <https://doi.org/10.2478/ama-2024-0048>
- Systemes, D. (2011). *Solidworks 2019*. Dessault Systemes: Vélizy-Villacoublay, France.
- Vachev, A. A. (1998). Synthesis and analysis of kinematic cutting schemes for rotating tool and workpiece. Plovdiv. Technical University – Plovdiv.
- Waguespack, C. (2014). *Mastering Autodesk Inventor 2015 and Autodesk Inventor LT 2015*: Autodesk Official Press. John Wiley & Sons.
- Waldron, K. J., & Schmiedeler, J. (2016). Kinematics. In *Springer handbook of robotics* (pp. 11-36). Cham: Springer International Publishing.